PI Controller Based Load Frequency Control Approach for Single-Area Power System Having Communication Delay

Sahaj Saxena * **Yogesh V. Hote** **

* *Electrical and Instrumentation Engineering Department, Thapar Institute of Engineering and Technology, Patiala, India (e-mail: sahajsaxena11@gmail.com).*
** *Department of Electrical Engineering, Indian Institute of Technology Roorkee, Roorkee, India (e-mail: yhotefee@iitr.ac.in)*

Abstract: The modern power systems are becoming complicated day by day because of the delays introduced by the communication networks. Due to this reason, the traditional load frequency control (LFC) design scheme depicts a destabilizing impact and an unacceptable performance. Therefore, this paper proposes an analytico-graphical approach for designing PI controller for a single-area LFC system having communication delay. The concept is based on extracting stability region in parameter space (k_p, k_i) with predefined gain and phase margins. Further, the values of optimal k_p and k_i are selected using integral error criterion. The proposed scheme gives faster disturbance rejection response as compared to the recently developed LFC scheme. The controller also works well when the system parameters are perturbed from their nominal values.

Keywords: Disturbance rejection, load frequency control, PI parameters, gain and phase margins, time delays.

1. INTRODUCTION

Traditionally, LFC is an ancillary service to regulate net scheduled power exchange and frequency fluctuations to meet load demand. See Ibraheem et al. (2005); Saxena and Hote (2013); Hanwate et al. (2018). However for effective implementation of LFC scheme, the present day power generation sector witnesses increased competition in deregulated market and huge demand of ancillary regulation services in more open, adaptable and distributed communication network. In such communication network, time delay arises during transmission of telemetry signals from phasor measurement units, power line carriers, remote terminal units to local control center, local controller to the generating unit, etc. These communication (time) delays may have destabilizing impact on the system dynamics and therefore degrades the system's performance. Thus, it is a serious problem and most of the research works on LFC have neglected such type of delay while formulating control laws. To address LFC scheme in presence of communication delays, few mathematically complex control strategies (such as Bevrani (2009); Yu and Tomsovic (2004); Jiang et al. (2012); Wang et al. (2015)) have been developed using linear matrix inversion and state feedback control.

In classical control theory, gain and phase margin (GPM) defines the robustness of the system in the sense that gain variation and phase delay do not lead to instability. Moreover, GPM also highlights the performance of closed-loop system in terms of relative stability and transient performance of the system response. Furthermore, minimizing the given integral error performance index (such as *IE, ISE, IAE*) makes the control system optimal. Therefore, keeping the aforementioned facts in mind, we propose a proportional integral (PI) controller based LFC scheme for single-area power system containing non-reheated turbine and communication delay in which for selection of PI parameters, the stability boundary locus (SBL) approach is utilized. The stability region in controller parameter space is determined with constraints on GPM and the controller parameters are selected on the basis of integral of error index (i.e., $IE = \int \epsilon(t)dt$ where $\epsilon(t)$ is the difference between input and output of control system). The proposed scheme regulates the frequency excursion in presence of sudden load efficiently. Moreover to the best of our knowledge, such control scheme has not been studied for LFC problem with communication delay so far.

The rest of the paper is organized as follows. Section 2 presents the encouragement to perform this study. In section 3, the proposed control strategy is described. Simulations are carried out to test the efficiency and efficacy of the control strategy in section 4. Finally section 5 concludes the present study.

2. MOTIVATION

The power system and control research find PI controller, the most acceptable controller for LFC analysis but in presence of communication delay, literature lacks some analytical, robust and optimal PI based LFC design. Also recently, a new PI controller tuning scheme via SBL to counter communications delay in LFC is proposed by Sönmez and Ayasun (2016), in which the stability regions are investigated in controller parameter space ($k_p - k_i$) plane. It is observed that in this technique there is a need to identify stable and unstable regions, (See $R1, R2, ..., R5$ in Fig. 2 of Sönmez and Ayasun (2016)). Further, it is shown that selecting any point in the stable region, the stabilizing parameter values of PI can be identified, but no selection criterion is described to pick the most appropriate stabilizing values of k_p and k_i parameters. Also, these stabilizing values do not ensure desired robustness and optimal performances. Therefore, the aforementioned points motivates us to develop an analytico-graphical control scheme that fulfills the research gaps in this direction.

3. PROPOSED CONTROL STRATEGY

3.1 Time-delayed LFC dynamics

We know that designing any controller on a single-machine power system (single-area) is logically the best place to begin an evaluation of the controller. Therefore, we present the standard simplified single-area LFC model in Fig. 1 in which the communication delay is expressed by an exponential function $e^{-\theta s}$, where θ gives the communication delay time; see Jiang et al. (2012). Here, all the communication delays are accumulated into single constant delay before controller as it is assumed that all the delays are identical and the control center waits to receive the telemetered values. Due to no net tie-line power exchange in the single-area LFC scheme, the area control error (ACE) is defined as

$$ACE(t) = \beta \Delta f(t)$$

where β is frequency bias constant. The PI controller $C(s)$ takes the form:

$$u(t) = -k_p ACE(t) - k_i \int ACE(t)dt$$

where k_p and k_i are proportional and integral gains, respectively. The approximated mathematical models in Fig. 1 are

$$P_G(s) = \frac{1}{sT_g + 1}$$

$$P_T(s) = \frac{1}{sT_{ch} + 1}$$

and

$$P_P(s) = \frac{1}{Ms + D}$$

where T_g, T_{ch}, M, D denote the governor time constant, turbine time constant, generator inertia constant, and damping coefficient, respectively. The complete model of power system (depicted by dotted block in Fig. 1) can now be written as:

$$P(s) = \frac{P_G(s)P_T(s)P_P(s)}{1 + (P_G(s)P_T(s)P_P(s)/R)}$$

where R is droop characteristics.

3.2 GPM based computation of PI parameters

Motivated by the elegant scheme of exploring stabilizing PI parameters in Tan et al. (2006), we produce a modified scheme which efficiently find the stability region based on desired GPM specification. We present our work with few definitions.

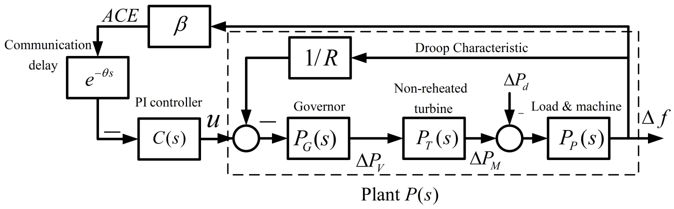

Fig. 1. Block diagram of single-area power system

Definition 1. For plant $P(s)$ with controller $C(s)$, the gain margin A and the phase margin ϕ are defined, respectively, as:

$$A = 1/|C(j\omega_p)P(j\omega_p)|$$

and

$$\phi = \arg [C(j\omega_g)P(j\omega_g)| + \pi$$

where ω_p and ω_g are given, respectively, by

$$\arg [C(j\omega_g)P(j\omega_g)] = -\pi$$

and

$$|C(j\omega_p)P(j\omega_p)| = 1$$

.

Definition 2. A GPM tester $Q(s) = Ae^{-j\phi}$ is a virtual compensator (practically non exist) provides information on plotting the boundary lines of constant A and ϕ in ($k_p - k_i$) parameter plane.

Definition 3. The stability domain $\mathbf{L}$ with its boundary $\mathcal{L}$ in the parameter space $\mathbf{S}$ with k_p, k_i being coordinates is a simple connected region such that for $(k_p, k_i) \in \mathbf{L}$, all the roots of characteristic equation $\Delta(s)$ lie in open left-half of the s-plane. This $\mathbf{L}$ segregates $\mathbf{S}$ into stable and unstable region.

In order to obtain the stabilizing PI parameters (k_p, k_i), the GPM tester is augmented before $C(s)$ as depicted in Fig. 2. Next to obtain the $\mathcal{L}$ of $\mathbf{L}$ in $\mathbf{S}$, we first obtain $\Delta(s)$ of closed-loop time-delayed LFC system in Fig. 2 as

$$\Delta(s) = M(s) + N(s)e^{\psi} \tag{1}$$

where $M(s) = m_4 s^4 + m_3 s^3 + m_2 s^2 + m_1 s$, $N(s) = n_1 s + n_0$, and $\psi = -\theta s - j\phi$. The coefficients of polynomials $M(s)$ and $N(s)$ are, $m_4 = RT_gT_{ch}M$, $m_3 = MRT_{ch} + RDT_gT_{ch} + RT_gM$, $m_2 = MR + RDT_{ch} + RT_gD$, $m_1 = RD + 1$, $n_1 = A\beta Rk_p$, $n_0 = A\beta Rk_i$. Now, to find $\mathbf{L}$ with $\mathcal{L}$ in $\mathbf{S}$ for specified GPM, we follow corollary 1.

Corollary 1. The PI parameters (k_p, k_i) for a given value of gain margin can be obtained by substituting $\phi = 0$ in $\Delta(s)$. Likewise, the controller parameters for given phase margin can be achieved by setting $A = 1$ in $\Delta(s)$.

Proof. See Appendix A

Therefore, for a fixed phase margin ϕ, we set $A = 1$ and by substituting $s = j\omega$ and expanding exponential term as $e^{j(\bullet)} = cos(\bullet) + jsin(\bullet)$ in (1), we get the characteristic equation as

$$\begin{aligned}\Delta^{\phi}(j\omega) =& (m_4\omega^4 - m_2\omega^2 + n_0^{\phi}cos\alpha - n_1\omega sin\alpha) + \\ & j(-m_3\omega^3 + m_1\omega + n_1^{\phi}\omega cos\alpha + n_0^{\phi}sin\alpha)\end{aligned} \tag{2}$$

where $\alpha = -\theta\omega - \phi$, $n_0^{\phi} = \beta k_i R$ and $n_1^{\phi} = \beta k_p R$. Similarly for fixed gain margin A, set $\phi = 0$ in (1), which gives

$$\begin{aligned}\Delta^{A}(j\omega) = & (m_4\omega^4 - m_2\omega^2 + n_0 cos\omega\theta + n_1\omega sin\omega\theta) \\ & +j(-m_3\omega^3 + m_1\omega + n_1\omega cos\omega\theta - n_0 sin\omega\theta)\end{aligned} \tag{3}$$

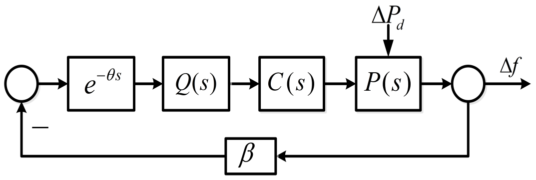

Fig. 2. Block diagram of LFC system with GPM tester

Equating the real and imaginary parts of (2) to zero, we get

$$\begin{aligned} -k_p X_1(\omega) + k_i Y_1(\omega) = Z_1(\omega) \\ k_p X_2(\omega) + k_i Y_2(\omega) = Z_2(\omega) \end{aligned} \tag{4}$$

where $X_1(\omega) = \beta R\omega sin(\alpha)$, $Y_1(\omega) = \beta Rcos(\alpha)$, $Z_1(\omega) = -m_4\omega^4 + m_2\omega^2$, $X_2(\omega) = \beta R\omega cos(\alpha)$, $Y_2(\omega) = \beta Rsin(\alpha)$, $Z_2(\omega) = m_3\omega^3 - m_1\omega$. Similarly for (3), we obtain

$$\begin{aligned} k_p X_3(\omega) + k_i Y_3(\omega) = Z_1(\omega) \\ k_p X_4(\omega) - k_i Y_4(\omega) = Z_2(\omega) \end{aligned} \tag{5}$$

where $X_3(\omega) = A\beta R\omega sin(\omega\theta)$, $Y_3(\omega) = A\beta Rcos(\omega\theta)$, $X_4(\omega) = A\beta R\omega cos(\omega\theta)$, $Y_4(\omega) = A\beta Rsin(\omega\theta)$. Now, on solving the two equations of (4), the stability locus for fixed phase margin $\mathcal{L}_\phi(k_p, k_i, \omega)$ in $(k_p - k_i)$ plane is obtained as

$$k_p = \frac{Y_1(\omega)Z_2(\omega) - Y_2(\omega)Z_1(\omega)}{X_1(\omega)Y_2(\omega) + X_2(\omega)Y_1(\omega)} \tag{6}$$

$$k_i = \frac{X_2(\omega)Z_1(\omega) + X_1(\omega)Z_2(\omega)}{X_1(\omega)Y_2(\omega) + X_2(\omega)Y_1(\omega)} \tag{7}$$

Likewise for (5), the stability locus for fixed gain margin $\mathcal{L}_A(k_p, k_i, \omega)$ in $(k_p - k_i)$ plane is obtained as

$$k_p = \frac{Y_4(\omega)Z_1(\omega) + Y_3(\omega)Z_2(\omega)}{X_3(\omega)Y_4(\omega) + X_4(\omega)Y_3(\omega)} \tag{8}$$

$$k_i = \frac{X_4(\omega)Z_1(\omega) - X_3(\omega)Z_2(\omega)}{X_3(\omega)Y_4(\omega) + X_4(\omega)Y_3(\omega)} \tag{9}$$

The pair of equations (6), (7) and (8), (9) produce desired GPM based $\mathcal{L}$ as ω runs from 0 to ∞.

Definition 4. Griding frequency ω_h denotes the frequency at which the imaginary part of $\Delta(s) = 0$ where $s = j\omega$. Basically, ω_h limits the value of ω upto which $\mathcal{L}$ is swiped out to form $\mathbf{L}$.

We also recall the corollary 2 to identify the region in the parameter space that would yield the parameter set k_p and k_i for stabilization of the control system.

Corollary 2. Tan et al. (2006). The line $k_i = 0$ and $\mathcal{L}$ together forms the region $\mathbf{L}$ in $\mathbf{S}$. $\mathbf{L}$ is a stable region if the arbitrary test point in that region yields the value of stabilizing k_p and k_i.

Proof. See Appendix B

Once the ω_h is obtained, there is no need to proceed further to draw locus in $\mathbf{S}$. The required ω_h for $\mathcal{L}_\phi$ and $\mathcal{L}_A$ can be obtained by substituting $k_i = 0$ in (7) and (9), respectively. After the stabilizing PI controller region is computed, our next goal is to select k_p and k_i values from the region $\mathbf{L}$ to achieve optimum performance. We know that for good disturbance rejection, the IE index for step disturbance or steady state error should be as low as possible. The following theorem helps to provide optimum PI parameters.

Theorem 1. For the disturbance rejection performance in PI design, $IE = \frac{\sigma}{k_i}$ for step disturbance input $\Sigma(s) = \frac{\sigma}{s}$, $\sigma \in \mathbb{R}^+$.

Proof. Let $\epsilon(s)$ be error corresponding to step input disturbance $\Sigma(s) = \frac{\sigma}{s}$ of the plant $G(s)$ arranged in unity feedback configuration with controller $C(s) = k_p + \frac{k_i}{s}$. Therefore, we can say

$$\epsilon(s) = \frac{G(s)}{1 + C(s)G(s)}\Sigma(s)$$

and

$$IE = \lim_{t\to\infty} \int_0^t \epsilon(\eta)d\eta = \lim_{s\to 0} \frac{G(s)\Sigma(s)}{(1 + C(s)G(s))} = \frac{\sigma}{k_i}$$

.

Theorem 1 states that the maximization of k_i is equivalent to the minimization of IE. Therefore, the point corresponding to the highest value of k_i within the stability region should be selected to show the optimality of the control scheme.

4. SIMULATION RESULTS

To illustrate the effectiveness of the proposed control strategy, we consider the LFC model whose parameters are given in Sönmez and Ayasun (2016) and $\theta = 2.28$s. Our main purpose is to determine the stabilizing values of k_p and k_i such that $\Delta(s)$ in (1) should be Hurwitz stable with desired gain and phase margins. Generally, the recommended ranges of gain and phase margins are, respectively, $2-5$ and $30^0 - 60^0$. Suppose, our desired gain and phase margins are $A \geq 3$ and $\phi \geq 30^0$, respectively, then we substitute $\phi = 30^0$ in (2), we get stability locus $\mathcal{L}_{\phi=30^0}$ for specific phase margin with griding frequency $\omega_h^\phi = 1.288$ in Fig. 3. Similarly, by substituting $A = 3$ in (3), we obtain $\mathcal{L}_{A=3}$ for specific gain margin with griding frequency $\omega_h^A = 1.47$. The common region covered by $k_i = 0$, $\mathcal{L}_{A=3}$ and $\mathcal{L}_{\phi=30^0}$ gives stability region of desired gain and phase margins. Now, on comparing the stability region ($\mathcal{L}_{SA}$) obtained using Sönmez and Ayasun (2016), the span of the shaded region in Fig. 3 is very less which reduces the computational search effort with desired stability margin. Now, we select a point near the boundary of $\mathcal{L}_{A=3}$ from shaded region in Fig. 3 (denoted by '+' mark in zoomed portion of Fig. 3), i.e., $k_p = 0.29, k_i = 0.109$. Using these values, the time response simulation of frequency deviation Δf for load increment $\Delta P_d(s) = 0.1$ p.u. at $t = 1$ s is shown in Fig. 4. The disturbance rejection performance is faster and non-oscillatory in comparison to the PI controller having parameters $k_p = 0.55, k_i = 0.55$ suggested in Sönmez and Ayasun (2016). Moreover, to measure the optimality of the proposed controller, the IE for proposed method is -9.17 whereas for Sönmez and Ayasun (2016), it is -1.82, which confirms the optimality of the proposed scheme.

In controller design and analysis, it is necessary that the controller not only maintain the system stability but also possess a strong robust performance. Therefore to judge the robust performance of the controller, the plant parameters and communication delay are varied from their nominal values. When each parameter of system is 20%

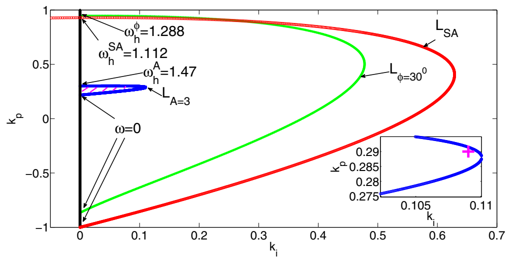

Fig. 3. Stability boundary region for PI controller

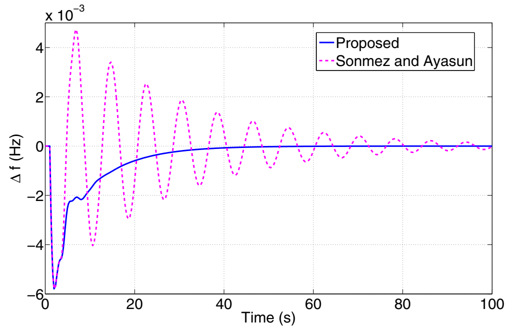

Fig. 4. Time response simulation for frequency deviation

increased then the proposed scheme in Fig. 5(a) stabilizes the frequency fluctuation whereas the response using Sönmez and Ayasun (2016) scheme is unstable. Similarly if the parameters are 20% decreased, the response in Fig. 5(b) is oscillatory before fluctuations die out by Sönmez and Ayasun (2016) scheme whereas the proposed scheme produce smooth response. Lastly, when communication delay is varied from $\theta = 2.28$ s to $\theta = 4$ s, the proposed scheme in Fig. 5(c) is capable to reject disturbance while Sönmez and Ayasun (2016) scheme destabilizes the system.

5. CONCLUSIONS

This paper proposes an analytico-graphical method of obtaining PI parameters which are based on SBL approach using specific gain and phase margins for single-area power systems having communication delay. The obtained results show that the designed controller can ensure good performance despite load disturbance and indeterminate delays in the communication network. Thus, the proposed scheme could be a benchmark solution for LFC design of multi-area as well as multi-machine power systems when delays are introduced by communication networks.

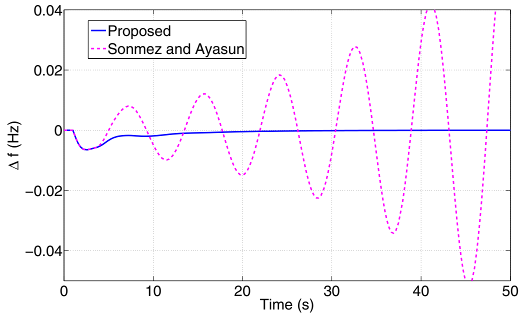

(a)

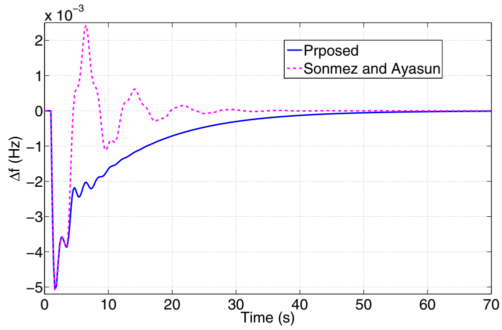

(b)

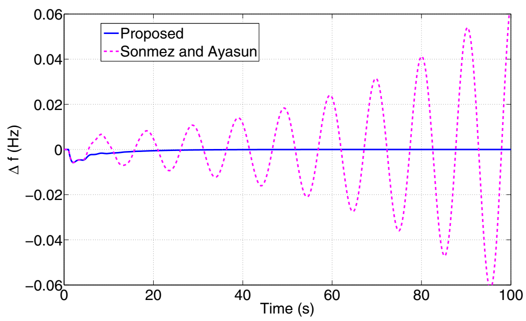

(c)

Fig. 5. Response of the system when all the plant parameters are (a) 20% increased, (b) 20% decreased, and (c) communication delay is varied in the nominal system

REFERENCES

Bevrani, H. (2009). *Robust power system frequency control.* Springer, New York.

Yu, X. and Tomsovic, K. (2004). *Application of linear matrix inequalities for load frequency control with communication delays.* IEEE Transactions on Power Systems, 19(3), 1508-1515.

Jiang, L., Yao, W., Wu, Q.H., Wen, J.Y. and Cheng, S.J. (2012) *Delay-dependent stability for load frequency control with constant and time-varying delays.* IEEE Transactions on Power Systems, 27(2), 932-941.

Wang, R., Li, X. and Zhou, W.Y. (2015). Guaranteed cost load frequency control for a class of uncertain power systems with large delay periods. *Neurocomputing*, 168, 269-275.

Sönmez, S. and Ayasun, S. (2016). Stability region in the parameter space of PI controller for a single-area load frequency control system with time delay. *IEEE Transactions on Power Systems*, 31(1), 829-830.

Jiang, L., Yao, W., Wu, Q.H., Wen, J.Y. and Cheng, S.J. (2012). Delay-dependent stability for load frequency control with constant and time-varying delays. *IEEE Transactions on Power Systems*, 27(2), 932-941.

Tan, N., Kaya, I., Yeroglu, C. and Atherton, D.P. (2006). Computation of stabilizing PI and PID controllers using the stability boundary locus. *Energy Conversion and Management*, 47(18), 3045-3058.

Saxena, S. and Hote, Y.V. (2013). Load frequency control in power systems via internal model control scheme and model-order reduction. *IEEE Transactions on Power Systems*, 28(3), 2749-2757.

Hanwate, S., Hote, Y.V. and Saxena, S. (2018). Adaptive Policy for Load Frequency Control. *IEEE Transactions on Power Systems*, 33(1), 1142-1144.

Ibraheem, Kumar, P., & Kothari, D.P. (2005). Recent philosophies of automatic generation control strategies in power systems. *IEEE Transactions on Power Systems*, *20*(1), 346-357.

Appendix A. PROOF OF COROLLARY 1

Consider a plant

$$G(s) = N(s)/D(s) \tag{A.1}$$

with PI controller $C(s) = k_p + k_i/s$ and GPM tester $Q(s) = Ae^{-j\phi}$. The closed-loop characteristic equation becomes

$$\Delta(s) = 1 + Ae^{-j\phi}(k_p + k_i/s)N(s)/D(s) \tag{A.2}$$

On substituting $\phi = 0$ in (A.2), we get the characteristic equation for fixed gain margin as

$$\Delta^A(s) = 1 + A(k_p + k_i/s)N(s)/D(s) \tag{A.3}$$

Equation (A.3) indicates that $\Delta^A(s)$ is free form phase margin term ϕ and only A is present. Similarly, on putting $A = 1$ in (A.2), we get the characteristic equation for fixed phase margin as

$$\Delta^\phi(s) = 1 + e^{-j\phi}(k_p + k_i/s)N(s)/D(s) \tag{A.4}$$

which depicts that only ϕ enforces constraints during evaluation of k_p and k_i parameters.

Appendix B. PROOF OF COROLLARY 2

We fragment $N(s)$ and $D(s)$ of (A.1) into their even and odd parts as

$$\begin{aligned} N(s) &= N_e(s^2) + sN_o(s^2) \\ D(s) &= D_e(s^2) + sD_o(s^2) \end{aligned} \tag{B.1}$$

Replace $s = j\omega$, in (B.1) and then substitute in (A.2), we get

$$\Delta(j\omega) = \Re(\Delta(j\omega)) + \Im(\Delta(j\omega)) \tag{B.2}$$

where

$$\begin{aligned} \Re(\Delta(j\omega)) = &-\omega^2 D_o(-\omega^2) - \omega^2 Ak_p N_o(-\omega^2) \\ & cos\phi - \omega Ak_p N_e(-\omega^2) sin\phi + Ak_i \\ & N_e(-\omega^2) cos\phi - \omega Ak_i N_o(-\omega^2) sin\phi \end{aligned} \tag{B.3}$$

and

$$\begin{aligned} \Im(\Delta(j\omega)) = &\omega D_e(-\omega^2) + \omega Ak_p N_e(-\omega^2) cos\phi - \\ & \omega^2 Ak_p N_o(-\omega^2) sin\phi + \omega Ak_i N_o(-\omega^2) \\ & cos\phi + Ak_i N_e(-\omega^2) sin\phi \end{aligned} \tag{B.4}$$

$\Delta(j\omega)$ becomes unstable at $s = j\omega$ when its roots cross the imaginary axis, i.e., (B.3) and (B.4) become zero simultaneously which implies $\omega = 0$ and $k_i = 0$. Thus, $\mathcal{L}$ and $k_i = 0$ together forms $\mathbf{L}$ that divides $\mathbf{S}$ into stable and unstable regions. Finally, when we select any point (k_p, k_i) within region, then the stable region $\mathbf{L}$ which includes the values of stabilizing k_p and k_i can be obtained.